

# **NGC 4593**

Untertitel (falls nötig)

Vorname Nachname

Universität XYZ

Betreuer: Dr. XYZ

July 4, 2025

## **Abstract**

Abstract

# Contents

<b>1</b>	<b>Introduction</b>	<b>5</b>
<b>2</b>	<b>Scientific Background</b>	<b>6</b>
2.1	Active Galactic Nuclei . . . . .	6
2.1.1	Structure of an AGN . . . . .	7
2.1.2	Classification . . . . .	9
2.1.3	Unification Model . . . . .	9
2.1.4	Spectral Features . . . . .	9
2.1.5	Variability . . . . .	11
2.2	Reverberation Mapping . . . . .	11
2.2.1	Principle . . . . .	11
2.2.2	Transferfunction . . . . .	12
2.2.3	Cross-Correlation Function . . . . .	12
2.2.4	Black-Hole Mass . . . . .	12
2.3	Bowen Fluorescence . . . . .	12
<b>3</b>	<b>Campaign and Analysis</b>	<b>13</b>
3.1	NGC4593 . . . . .	13
3.2	2016 Campaign by E. M. Cackett . . . . .	13
3.3	Intercalibration . . . . .	14
<b>4</b>	<b>Reverberation Analysis of NGC4593</b>	<b>15</b>
4.1	AVG- and RMS-Spectrum . . . . .	15
4.2	Lightcurves . . . . .	15
4.2.1	Continua . . . . .	15
4.2.2	Emission Lines . . . . .	15
4.3	Line Profiles . . . . .	15
4.4	Cross-Correlation Function . . . . .	15
4.5	Time Lag and BH Masses . . . . .	15

4.6	Bowen Fluorescence . . . . .	15
<b>5</b>	<b>Discussion</b>	<b>16</b>

# List of Figures

2.1	Different components of an AGN. Adapted from Mo, Bosch, and White (2010) Figure 14.3. . . . .	7
2.2	Unification model of an AGN (Fermi Gamma-ray Space Telescope 2025). . . . .	10
3.1	A DSS image of NGC4593. . . . .	13

# List of Tables

3.1 Overview of STIS Grating Characteristics (Space Telescope Science Institute 2025) . . . . .	14
----------------------------------------------------------------------------------------------------	----

# 1. Introduction

## 2. Scientific Background

This chapter provides a theoretical background for the topics addressed in this thesis. It introduces the fundamental physical processes and structures of Active Galactic Nuclei (AGN), with a particular focus on the properties of the Broad-Line Region (BLR), which plays a central role in this work. The concept of AGN unification, the different observational classifications, and the variability of AGN are outlined. Furthermore, reverberation mapping is discussed in detail, as it serves as the main analysis method in this thesis. It is a powerful tool to probe the geometry and kinematics of the BLR and to estimate the mass of the central supermassive black hole. In the final section of this chapter, an overview of Bowen fluorescence is provided, as this process may account for some spectral features that will be discussed in the following analysis.

### 2.1 Active Galactic Nuclei

What are Active Galactic Nuclei (AGN)? They represent a class of galaxies that are among the brightest and most energetic objects in the known universe, with bolometric luminosities ranging from  $10^{41}$  to  $10^{48}$  erg s $^{-1}$ , surpassing typical galaxies by many orders of magnitude (Bradley M. Peterson 1997). This enormous emission originates from the central region of the AGN, which outshines the stars of its so-called host galaxy. It is powered by matter accreting onto the central supermassive black hole (SMBH) in the form of an accretion disk (Shakura and Sunyaev 1973). To better understand the physical nature of AGN, it is important to examine their observational characteristics and internal structure. AGN emit radiation across the entire electromagnetic spectrum, and their spectral features provide crucial information about the physical conditions and kinematics in the central regions. The following sections present the main components of AGN, introduce the unification model that links different AGN types, and describe commonly used classification schemes. Particular attention is given to the variability of AGN, which plays a central role in the reverberation mapping analysis carried out in this thesis.



### 2.1.1 Structure of an AGN

The structure of an AGN consists of several distinct components, as illustrated in Figure 2.1. These include a central supermassive black hole (SMBH), an accretion disk that feeds the SMBH, a surrounding dusty torus, and ionized gas regions known as the broad-line region (BLR) and narrow-line region (NLR). In some AGNs, powerful relativistic jets are launched perpendicular to the accretion disk. However, these jets will not be discussed further in this section, as they are not relevant to the scope of this thesis. Each of the components contributes differently to the observed spectrum of the AGN, as will be discussed in more detail in Section 2.1.4.

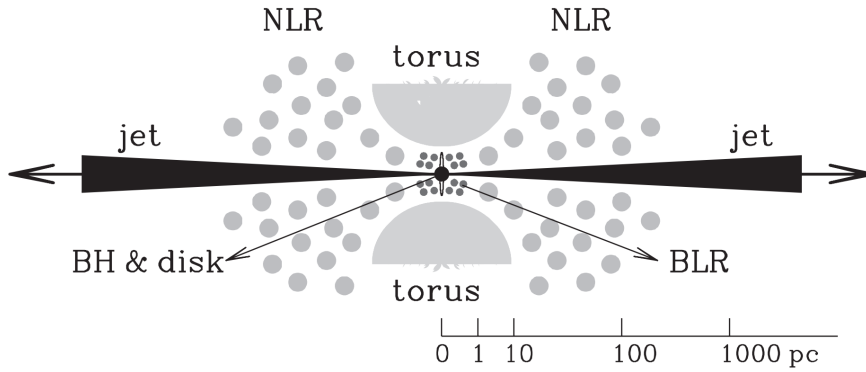


Figure 2.1: Different components of an AGN. Adapted from Mo, Bosch, and White (2010) Figure 14.3.

#### Supermassive Black Hole and Accretion Disk

The center of an AGN is occupied by a supermassive black hole (SMBH), with masses typically ranging from  $10^6 M_{\odot}$  to more than  $10^{10} M_{\odot}$ . While the SMBH itself does not emit radiation, it dominates the gravitational potential in the innermost regions and acts as the central engine driving all observed AGN phenomena. Gas from the surrounding accretion disk slowly spirals inward toward the SMBH due to angular momentum transport driven by viscosity inside the disk. During this process, gravitational potential energy is converted into heat, causing the disk to reach very high temperatures. As a result, a significant fraction of the gravitational energy of the matter is transformed into thermal radiation, which accounts for the enormous luminosity observed in AGNs (Netzer 2013).

The accretion disk itself is a geometrically thin and optically thick structure composed of ionized gas in differential rotation around the SMBH (Shakura and Sunyaev 1973). The disk's composition is primarily ionized hydrogen and helium, with traces

of heavier elements (Netzer 2013). It extends from the innermost stable circular orbit (ISCO) near the event horizon out to distances of several light-days, where the temperature drops and dust can survive. The radial extent of the disk is relatively small on galactic scales, typically ranging from a few light-hours to a few light-days, corresponding to about  $10^{-3}$  to  $10^{-2}$  pc (Netzer 2013; Hickox and Alexander 2018). The hottest regions are located in the innermost part of the disk, with typical temperatures ranging from  $10^4$  to  $10^5$  K (Hickox and Alexander 2018).

### **Broad-Line and Narrow-Line Region**

Outside the accretion disk lies a distribution of photoionized gas clouds that give rise to the characteristic emission lines observed in AGN spectra. The innermost of these is the broad-line region (BLR), located at distances of a few light-days to light-weeks from the central SMBH. The BLR consists of dense gas clouds (electron densities  $n_e \sim 10^9\text{--}10^{11} \text{ cm}^{-3}$ ) moving at high velocities of several thousand kilometers per second due to the strong gravitational influence of the black hole (Netzer 2013). These velocities lead to significant Doppler broadening of permitted emission lines and line widths of several thousand km/s. The BLR is primarily photoionized by the continuum radiation emitted from the accretion disk.

Further out lies the narrow-line region (NLR), which extends over scales of hundreds to thousands of parsecs. The gas in this region is less dense ( $n_e \sim 10^2\text{--}10^6 \text{ cm}^{-3}$ ) and moves at much lower velocities (a few hundred km/s), resulting in narrow emission lines with widths typically below 1000 km/s. In contrast to the BLR, the NLR emits both permitted and forbidden lines, which gets excited by collision and can only form in low-density environments. The NLR is often spatially resolved in nearby AGNs and is photoionized by the central source, although additional ionization from shocks may also contribute in some cases (Hickox and Alexander 2018; Netzer 2013).

Both the BLR and NLR serve as important diagnostics of the AGN structure and provide key information about gas dynamics, ionization mechanisms, and the orientation-dependent appearance of the active nucleus.

### **Dusty Torus**

Surrounding the accretion disk and broad-line region is the dusty torus, a geometrically thick and optically dense structure composed of gas and dust. It extends from the sublimation radius, where dust can survive the intense radiation of the accretion disk, out to scales of a few parsecs. The torus likely has a clumpy distribution and plays a crucial role in the unified model of AGNs which will be discussed in a later section. Dust within the torus absorbs high-energy radiation and re-emits it

thermally in the infrared. (Netzer 2013; Hickox and Alexander 2018).

### 2.1.2 Classification

AGNs can be broadly grouped into so called Seyfert galaxies, quasars and radio galaxies. Seyfert galaxies are further subdivided, based on the width of their optical emission lines and radio properties. Seyfert 1 Galaxies show broad emission lines, while Seyfert 2 Galaxies show only narrow emission lines, narrow-line Seyfert 1 galaxies (NLS1), low-ionization nuclear emission-line regions (LINERs), and BL Lac objects or blazars (Antonucci 1993; Urry and Padovani 1995).

### 2.1.3 Unification Model

Figure 2.2 shows the unification model of an AGN. As illustrated an AGN is powered by a supermassive black hole surrounded by several distinct regions. Closest to the black hole is the accretion disc, whose hot, optically thick gas emits the thermal “Big Blue Bump” in the optical/UV bands (Bradley M. Peterson 1997). Encircling the disc is the Broad-Line Region (BLR), a compact area of dense clouds orbiting at thousands of kilometers per second, which produces the broad emission lines. Outside the BLR lies the dusty torus, a toroidal structure of cooler gas and dust that can obscure the inner regions when viewed edge-on (Antonucci 1993). Beyond the torus, the more extended Narrow-Line Region (NLR) emits narrower lines from slower gas at distances of hundreds of parsecs. In radio-loud AGN, powerful relativistic jets emerge perpendicular to the disc plane, accelerating particles to near-light speeds and generating strong radio emission (Urry and Padovani 1995).

### 2.1.4 Spectral Features

AGNs emit radiation across the entire electromagnetic spectrum. A typical AGN exhibits strong X-ray and radio emission, as well as non-stellar ultraviolet and optical continua, along with both broad and narrow emission lines. However, not every AGN displays all of these features, as will be discussed in more detail later (Bradley M. Peterson 1997).

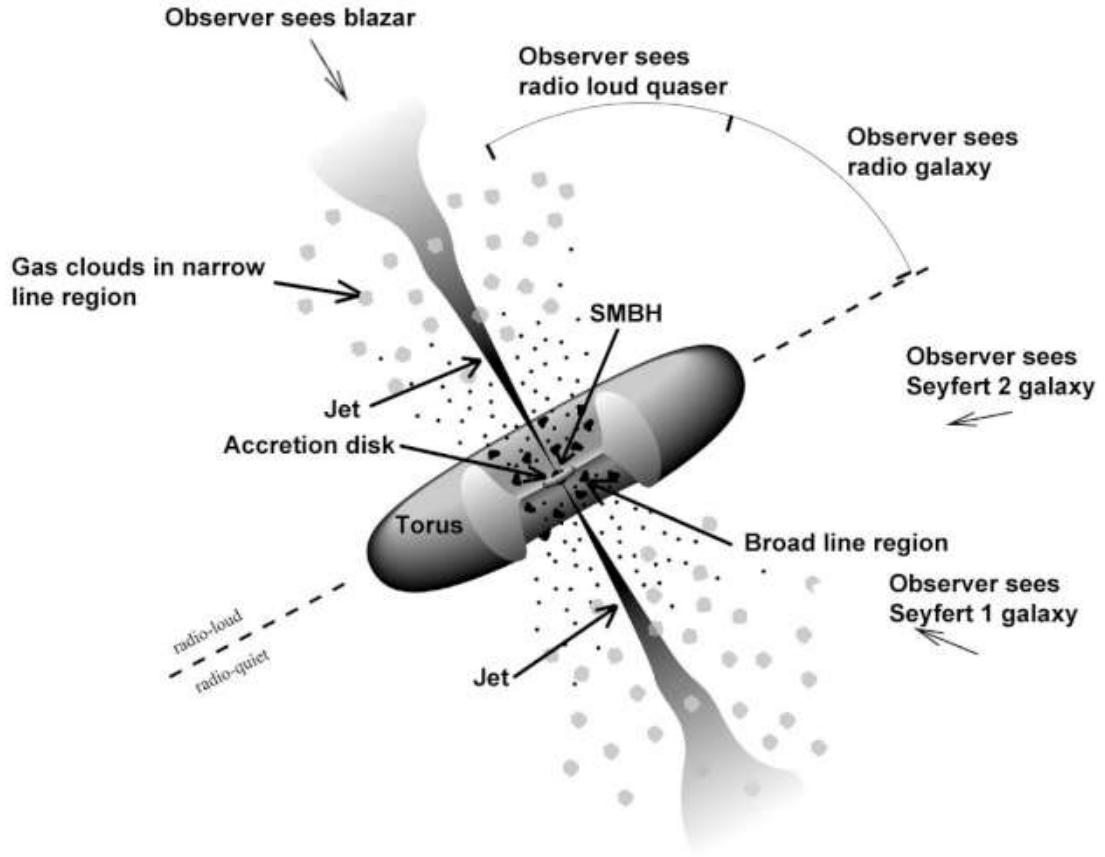


Figure 2.2: Unification model of an AGN (Fermi Gamma-ray Space Telescope 2025).

### Non-stellar Continuum Emission

AGNs typically have a strong, non-stellar continuum emission. In the optical and ultraviolet range, the spectrum often follows a power-law shape instead of a black-body curve, which implies a non-thermal origin. A noticeable feature in this part of the spectrum is the so-called *big blue bump*, a broad increase in emission that peaks in the ultraviolet between about 1000 and 3000 Å. It is thought to be caused by thermal radiation from the hot inner part of the accretion disk around the super-massive black hole (Bradley M. Peterson 1997; Osterbrock 1989). The shape and strength of this bump can give information about how fast matter is falling into the black hole.

Additionally, the ionized photons, emitted by the continuum, are responsible for exciting the gas clouds around the nucleus, which leads to emission lines in AGN spectra (Osterbrock 1989).

**Broad Emission Lines**

**Narrow Emission Lines**

**Infrared Emission**

**X-ray Emission**

**Radio Emission**

### **2.1.5 Variability**

## **2.2 Reverberation Mapping**

### **2.2.1 Principle**

The main focus of this work was to perform a classic reverberation analysis of NGC 4593, with a focus on the broad line region (BLR) and its geometry around the central supermassive black hole (SMBH).

This type of analysis aims to measure the time lag  $\tau$  between the variable continuum and the emission line response, in order to determine the spatial scale and structure of the BLR. By observing these variations over time and analyzing the delayed response of the broad lines, it is possible to learn more about the geometry and dynamics of the BLR and to estimate the mass of the SMBH.

Reverberation mapping (RM) is based on the strong correlation between a variable continuum emission  $C(t)$  and the emission line flux  $L(\nu, t)$  (Horne et al. 2021). This correlation originates from the photoionization of gas clouds in the BLR by the central continuum source. As the continuum changes, the emission lines react in a similar way, but with a time delay  $\tau$ , because of the distance between the central source and the BLR. This delay corresponds to the time it takes for light to travel from the central source to the BLR.

**2.2.2   Transferfunction**

**2.2.3   Cross-Correlation Function**

**2.2.4   Black-Hole Mass**

**2.3   Bowen Fluorescence**

## 3. Campaign and Analysis

The Analysis of this campaign bases of the observation campaign of NGC4593 in 2016 by Edward M. Cackett (Edward M Cackett et al. 2018). The observations took place between the 12th of July and the 6th of August with 26 successful observations and was performed with the Hubble Space Telescope (HST) using the Space Telescope Imaging Spectrograph (STIS). The following section will cover important properties of NGC4593 and the 2016 campaign.

### 3.1 NGC4593

NGC4593 is an active galactic nuclei (AGN), classified as an Seyfert 1 Galaxy with a Sb D morphology. It is located at RA = 12:39:39.44, DEC = -05:20:39.03 (2000) and has a of  $z = 0.0083 \pm 0.0005$  This correspond to a distance of about 35.6 MPc (SIMBAD 2025)based on the  $\Lambda$ CDM-Model.

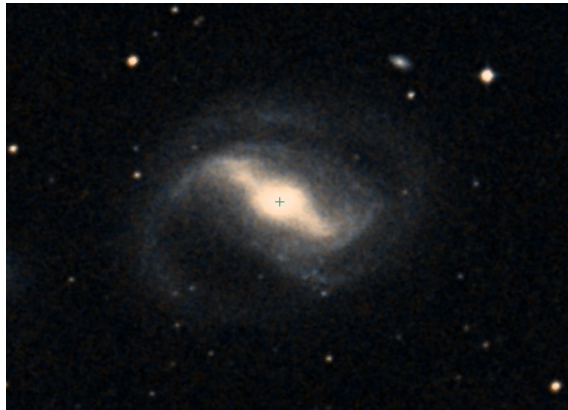


Figure 3.1: A DSS image of NGC4593.

### 3.2 2016 Campaign by E. M. Cackett

E. M. Cackett's campaign was designed to study wavelength dependent continuum lags. Therefore, the STIS instrument on the Hubble Space Telescope was used

with low-resolution gratings to measure a broad range of wavelengths. In each observation, spectra were taken using three different gratings: G140L, G430L, and G750L. These were used together with the  $52'' \times 0.2''$  slit.

The characteristics of the STIS gratings used in this analysis are summarized in Table 3.1.

Table 3.1: Overview of STIS Grating Characteristics (Space Telescope Science Institute 2025)

<b>Grating</b>	<b>Range [Å]</b>	<b>Exp. Time [s]</b>	<b>Res. Power</b>	<b>Dispersion [Å/pixel]</b>
G140L	1119–1715	1234	$\sim 1000$	0.6
G430L	2888–5697	298	$\sim 500 - 1000$	2.73
G750L	5245–10233	288	$\sim 500 - 1000$	4.92

### 3.3 Intercalibration



## 4. Reverberation Analysis of NGC4593

### 4.1 AVG- and RMS-Spectrum

### 4.2 Lightcurves

#### 4.2.1 Continua

#### 4.2.2 Emission Lines

### 4.3 Line Profiles

### 4.4 Cross-Correlation Function

### 4.5 Time Lag and BH Masses

### 4.6 Bowen Fluorescence

## 5. Discussion

# Bibliography

- Antonucci, Robert (1993). “Unified models for active galactic nuclei and quasars”. In: *Annual Review of Astronomy and Astrophysics* 31, pp. 473–521. DOI: 10.1146/annurev.aa.31.090193.002353.
- Cackett, Edward M et al. (2018). “Accretion disk reverberation with Hubble space telescope observations of NGC 4593: evidence for diffuse continuum lags”. In: *The Astrophysical Journal* 857.1, p. 53.
- Fermi Gamma-ray Space Telescope (2025). *Figure 1: Spectral Energy Distribution of an AGN*. URL: <https://fermi.gsfc.nasa.gov/science/etev/agn/figure1.jpg> (visited on 06/19/2025).
- Hickox, Ryan C. and David M. Alexander (2018). “Obscured Active Galactic Nuclei”. In: *Annual Review of Astronomy and Astrophysics* 56, pp. 625–671. DOI: 10.1146/annurev-astro-081817-051719. arXiv: 1806.04680 [astro-ph.GA].
- Horne, Keith et al. (2021). “Space telescope and optical reverberation mapping project. IX. velocity–delay maps for broad emission lines in NGC 5548”. In: *The Astrophysical Journal* 907.2, p. 76.
- Mo, Houjun, Frank van den Bosch, and Simon White (2010). *Galaxy Formation and Evolution*. Cambridge University Press. ISBN: 9780521857932.
- Netzer, Hagai (2013). *The Physics and Evolution of Active Galactic Nuclei*. Cambridge: Cambridge University Press.
- Osterbrock, Donald E. (1989). *Astrophysics of Gaseous Nebulae and Active Galactic Nuclei*. Mill Valley, California: University Science Books. ISBN: 9780935702111.
- Peterson, Bradley M. (1997). *An Introduction to Active Galactic Nuclei*. Cambridge University Press. ISBN: 9780521473484.
- Shakura, N. I. and R. A. Sunyaev (1973). “Black holes in binary systems. Observational appearance”. In: *Astronomy and Astrophysics* 24, pp. 337–355.
- SIMBAD (2025). *NGC4593*. URL: <https://simbad.u-strasbg.fr/simbad/sim-id?Ident=NGC4593> (visited on 06/10/2025).

- Space Telescope Science Institute (2025). *STIS Instrument Handbook: Gratings*. URL: <https://hst-docs.stsci.edu/stisihb/chapter-13-spectroscopic-reference-material/13-3-gratings> (visited on 05/12/2025).
- Urry, C. Megan and Paolo Padovani (1995). “Unified Schemes for Radio-Loud Active Galactic Nuclei”. In: *Publications of the Astronomical Society of the Pacific* 107.715, pp. 803–845. DOI: 10.1086/133630.